Proceedings of the 17th World Congress
The International Federation of Automatic Control
Seoul, Korea, July 6-11, 2008

A System for Automated Final Quality Assessment in the Manufacturing of Vacuum Cleaner Motors

Uroš Benko *, **Janko Petrovčič** *, **Bojan Mussiza** *, **Đani Juričić** *,[1]

* *Department of Systems and Control, Jožef Stefan Institute, Ljubljana, Slovenia*

Abstract: In this paper we present a system for fault detection and isolation of electrical motors for vacuum cleaners, which serves for on-line quality assessment at the end of the production line. The main focus of the paper is on detection of incipient mechanical faults by means of sound analysis. A detailed description of the procedures for detection and isolation of faults with mechanical origin is given. One of the contributions concerns innovative implementation of the feature extraction algorithm in a way that spectral procedures used in system analysis are substituted by much simpler and computationally more effective algorithms. Herewith the system is able to accurately isolate three different types of mechanical faults. Additional contribution regards diagnostic system integration which generates highest product end quality and traceability. In order to fully utilize a huge amount of diagnostic data, possibilities for the upgrade of the present diagnostic system with advanced production line supervision support are indicated.

1. INTRODUCTION

Fault diagnosis of electrical machines and rotating machinery is a thoroughly studied subject with numerous applications resulting thereof. The most widely used diagnostic means employ traditional techniques such as vibration analysis, analysis of electrical current and model-based parity relations (see Edwards et al. [1998] for a broad overview). These techniques proved useful in most cases in which various DC and AC drives, including universal motors were employed. Indeed, vibrations and current signal carry rich information about tiniest defects in mechanical parts such as imbalance, bearings, impacts etc. In this paper attention will be focused on a family of small universal motors with serially connected stator and rotor windings. For these types of motors the aforementioned techniques fail to provide reliable diagnosis of all relevant defects. Therefore, an alternative approach is addressed in this paper, which employs acoustic analysis. This resulted in the design and implementation of a diagnostic system for vacuum cleaner motors at the end of the production line. Indeed, various faults can occur during the assembly process such as insufficiently balanced rotational parts, improperly built-in bearings, missing contacts on commutator bars, deformations on fan impeller etc. These faults manifest in different ways, most notably in increased vibrations, unfamiliar sound, intensive sparking and howling. Therefore, a thorough test is required in order to gain a clear indication about tentative fault sources.

Similar motivation, though with different realisations, has been reported by several other authors and manufacturers. For example, the system produced by the company Schenck [2007], make use of vibration analysis, statistics and analytical redundancy based on the mathematical model. Similar approaches were utilised by Benning [2007] and Albas et al. [2006], but none of them employs sound analysis. Designed to be operable for a general class of electrical motors, these commercial systems fail to feature full range fault detectability and isolability. For example, geometry defects on the fan-impeller which result in unpleasant sound, are not addressed at all. Yet difficulties may be expected when more specific families of electrical motors have to be diagnosed. For example, the motor treated in this paper consists of rotor and stator windings connected serially. Serial connection results in high electric inductivity, which strongly attenuates higher-frequency components of the current signal. That is why any change in load, which should reflect in the current variation, remains unseen. For example, faulty bearing in this particular motor cannot be efficiently detected from the motor current signal. This is not an issue in motors with permanent magnet, where faulty bearings can be successfully detected by motor current analysis (Vetter et al. [1994]). Vibration analysis also falls short of expectations for two reasons. Firstly, in vibration measurement the vibration sensor should be placed as close as possible to the vibration source (e.g. faulty bearing), because magnitudes of vibrations decrease quickly with the distance from the source. In large machines, with large bearings, it is not a problem to mount a piezo sensor on the bearing housing. The dimensions of the motor represent additional constraints in the case of vacuum cleaner motors described below. Indeed, such a motor is rather small so that the sensor can reach only one bearing while the other bearing lies within the construction and is inaccessible. Another problem related to vibration analysis is that during lower rotational speeds the bearings provoke very weak vibrations, which cannot be detected by a vibration sensor,

[1] e-mail: dani.juricic@ijs.si

whilst during higher speeds the airflow of the fan impeller strikes the housing and provokes housing vibrations, which predominate vibrations originating by bearings. On the contrary, faulty bearings produce significant sound. Owing to the motor structure, the motor cover performs as a kind of resonator, which amplifies the sound from bearings and thereby makes the sound a representative means for fault detection.

The limitation above provided a strong motivation to address the problem of the diagnosis of mechanical faults in an alternative way based on sound analysis. This unique feature makes the system applicable to a much broader class of vacuum cleaner motors compared to those of the competitors. A thorough analysis of the fault detection and isolation algorithms has been presented in Benko et al. [2005]. A laboratory prototype of the diagnostic system has been constructed first. It proved indispensable for generating the requirements analysis and specification of the industrial version. In what follows the priorities are shifted from analysis of the diagnostic sources to the production issues concerning time efficient diagnostic algorithms capable of keeping the test cycle short, motor handling and HMI interface.

The paper is organized as follows. In the second section a detailed description of the procedures for detection of mechanical faults based on sound analysis is presented. In the third section an overview of the entire diagnostic system is presented. Section four discusses possible upgrades and integration into the production supervision system.

2. DIAGNOSIS OF MECHANICAL FAULTS: INDUSTRIAL SOLUTION

2.1 Faults implying noise

The most typical mechanical faults in the underlying motor (figure 1) are bearing faults and rubbing between the rotating and static parts. Both of these two faults have in common the fact that the emitted sounds contain high frequency repetitive bursts (see figure 2).

Fig. 1. The vacuum cleaner motor has a plastic housing, which enables smaller dimensions and impedes copying by the competition. The basic characteristics are: nominal speed-800Hz, voltage-230V, power-1.6kW.

In the case of bearing fault, the frequency content of bursts lies between 2.5kHz and 3.5kHz, whereas in the case of rubbing this frequency is much higher and lies between 10kHz and 15kHz (see figure 3). For the purpose of fault detection, one has to infer the repetition frequency of bursts. In the case of a bearing fault, the bursts repetition frequency depends on the bearings geometry, rotational speed and exact location of the fault within the bearing. For a given motor these frequencies read as follows:

- outer race defect: 2.6 f_0
- inner race defect: 4.4 f_0
- ball defect: 1.77 f_0

where f_0 denotes the rotational speed of the motor. In motors with rubbing, this frequency is usually f_0 and $2f_0$. This can be explained with the fact that in most cases rubbing occurs in one or two particular angular positions of the rotor, which in terms of frequency response means once or twice per rotor revolution. Since the frequency contents of bursts and the bursts repetition frequencies differ for these two faults, they can be clearly distinguished.

The signal with repetitive bursts can be treated as an amplitude modulated signal where the bursts repetition frequency corresponds to the modulation frequency, and the frequency content of bursts to the carrier frequency. Detection of bursts repetition frequency can therefore be done by using envelope analysis. Randall [2002] has shown that detection of repetition frequency of bursts from the signal envelope is much more robust to variations in rotational speed than detection from the original signal. Generally, the signal envelope is obtained by amplitude demodulation realized with Hilbert Transform (HT), Randall [1987]. HT is usually computed by means of Fourier transform. To accelerate the detection procedure, Hilbert Transform is replaced by a much simpler and faster routine, i.e. based on analysis of the absolute value of the signal. More details can be found in appendix A.

Figure 2 shows time signals, their spectra and the spectra of their envelopes for three motors with different bearing faults and a fault-free motor (case a). Obviously, the corresponding envelope spectra contain clear peaks at characteristic frequencies.

Detection of Bursts Repetition Frequency

In order to detect motors with bearing faults and motors with "rubbing" , the procedure depicted on figure 4 is employed. The original sound signal is firstly passed through two parallel bandpass filters. The first filter serves to isolate part of the signal excited by faulty bearing, whereas second filter isolates the sound emitted by possible rubbing. Secondly, the absolute value of the filtered signals is taken to extract their envelopes. Thus on the output of this module we get two envelopes. The first envelope corresponds to the bearing fault and the second one to the rubbing fault. The envelopes are then passed through the filters, which isolate only the frequencies characteristic for bearing fault and rubbing fault. The RMSs of these signals serve as the features for bearing fault F_B and rubbing fault F_R.

2.2 Faults implying aerodynamical noise

In the nominal operating conditions most of the emitted sound is due to aerodynamics. This is typical of such type of rotating machines. This sound depends on the geometry of the fan impeller and rotational speed. The higher the rotational speed, the greater is the sound intensity.

Even slight deviations in geometry of the fan impeller can substantially affect the sound, making it rather unpleasant

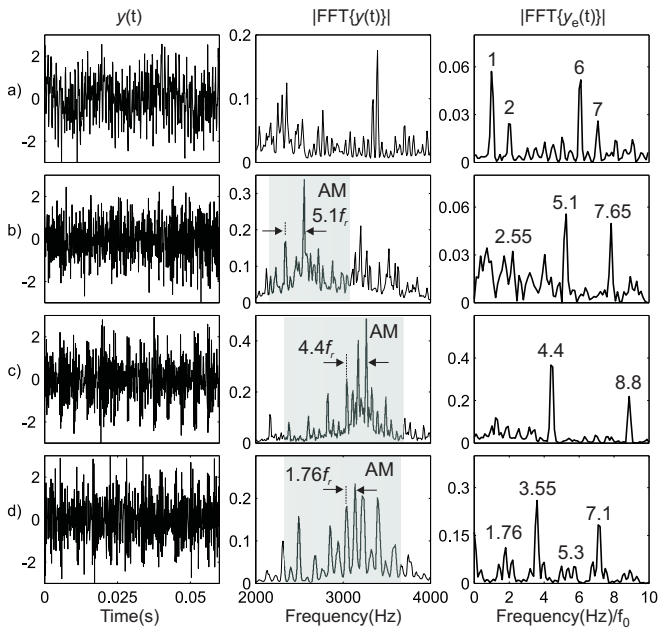

Fig. 2. The comparison of time signals $y(t)$ of four electrical motors, their amplitude spectra $|FFT\{y(t)\}|$ and spectra of their envelopes $|FFT\{y_e(t)\}|$. The motors have different rolling element bearing condition: a) fault-free bearing, b) outer race defect, c) inner race defect and d) ball defect. In cases b), c) an d) the spectra of signal envelopes contain clear peaks at the characteristic frequencies.

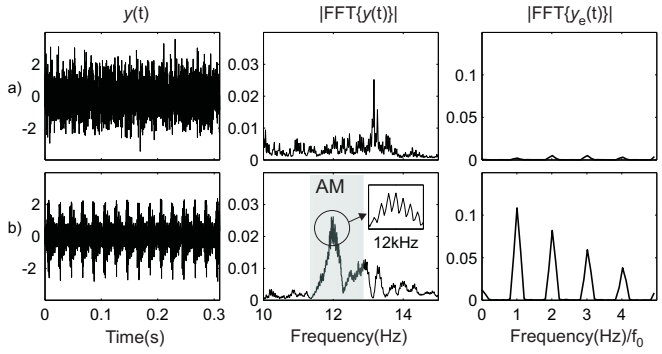

Fig. 3. The comparison of time signals $y(t)$ of two electrical motors, their amplitude spectra $|FFT\{y(t)\}|$ and spectra of their envelopes $|FFT\{y_e(t)\}|$. The motor in case a) is fault-free, whereas the motor in case b) is with the rubbing fault. In b) case the specter of envelope contains characteristic frequencies.

and annoying. It was found out that such faults imply increased power density at the frequencies kN_Sf_0, $k = 1, 2, ..$ and kN_Cf_0, k=1,2, where $N_S = 9$ is the number of shovels and $N_C = 16$ is the number of compartments in the diffuser. The important fact here is that these frequencies alone do not cause the annoying noise. The annoying noise is caused by the interplay between two frequencies $(16f_0, 18f_0)$. The frequency component at $16f_0$ is the noise resulting from the diffuser and $18f_0$ is noise caused by the shovels. This is beating phenomenon. Beating is a periodic pulsation of the loudness of a sound at a rate

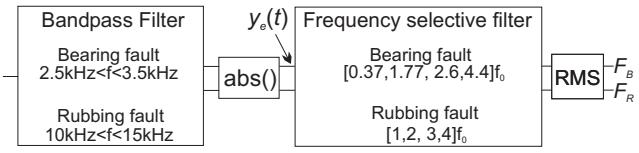

Fig. 4. Procedure for extraction of features for bearing F_B and rubbing fault F_R.

equal to the frequency difference between two very close harmonics. Whether or not beating is heard depends upon the amplitude of the harmonics in question and a variety of other factors whose discussion is beyond the scope of this work.

Detection of beating phenomenon

In order to detect motors that produce annoying aerodynamical noise due to the beating phenomenon, the procedure depicted in figure 5 is employed. The original sound signal $y(t)$ is first passed through the high-pass filter with cut-off frequency $f = 4.5f_0$. Herewith, the first four harmonics $[1-4]f_0$ are filtered out. Then, the filtered signal $y_F(t)$ is squared to obtain $y_F^2(t)$. Next, frequency selective filter is used to isolate the 1^{st} and 2^{nd} harmonic of the beating frequency. The RMS of the filtered signal is taken as a feature F_A for faults that produce annoying aerodynamical noise.

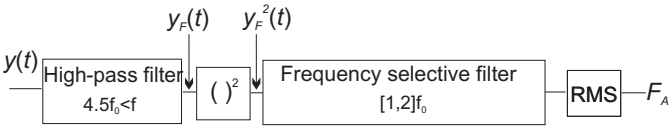

Fig. 5. Procedure for extraction of the feature F_A for faults that produce aerodynamic noise.

The following demonstration case serves as an additional explanation to the procedure in figure 5. Let us assume that signal consists of N sine waves, i.e. $y(t) = \sum_{i=1}^{N} a_i \sin(2\pi f_i t)$ where $f_i < f_j$ for each $i < j$. After filtering with highpass filter, all frequencies bellow the cut-off frequency are filtered out. Let us assume that there are $k-1$ such components. The filtered signal can be written as $y_F(t) = \sum_{i=k}^{N} a_i \sin(2\pi f_i t)$. The squared signal $y_F^2(t)$ reads as

$$y_F^2(t) = \sum_{i=k}^{N} \frac{a_i^2}{2} + \frac{1}{2}\sum_{i=k}^{N}\sum_{j=k}^{N} a_i a_j \cos(2\pi(f_i - f_j)t) -$$
$$-\sum_{i=k}^{N} \frac{a_i^2}{2}\cos(2\pi 2 f_i t) - \frac{1}{2}\sum_{i=k}^{N}\sum_{j=k}^{N} a_i a_j \cos(2\pi(f_i + f_j)t) \ .$$

A frequency selective filter will retain only the components

$$\frac{1}{2}\sum_{i}\sum_{j} a_i a_j \cos(2\pi(f_i - f_j)t)$$

for all i and j that satisfy $|f_i - f_j| \cong f_0$ and $|f_i - f_j| \cong 2f_0$. Herewith, the beating components are isolated. The strength of the beating depends on the amplitudes of the respective components a_i in a_j.

3. DIAGNOSTIC SYSTEM ARCHITECTURE

The diagnostic system is composed of five major parts (figure 6):

- 3 measurement and diagnostic stations,
- controller for mechanical handling of the motors and
- data acquisition (DA) system.

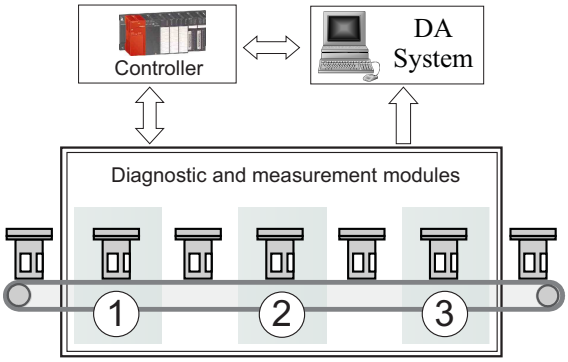

Fig. 6. The structure of a diagnostic system for quality assessment.

The system operation relies on direct measurements of 9 electrical and mechanical quantities i.e. power supply voltage, current, air pressure difference on the motor, revolution speed, electric power, vibrations, sound, air temperature and humidity. The last two variables are needed for various data conditioning. The quality assessment tasks are performed within three measurement modules running in parallel.

The control unit is built around the Mitsubishi MELSEC-Q PLC which takes care of mechanical handling and synchronization of tasks. The test cycle of the diagnostic system is adapted to the cycle of the assembly line, which is 9s. On the basis of data from the position sensors and pneumatic actuators, the control system generates signals for motor positioning, motor start-up and shut-down within the test. In addition, it takes care of transport of the motors through the diagnostic system.

The data acquisition system is based upon National Instrument NI 6220 and NI 6221 data acquisition modules. It is connected to the controller unit via RS 232 communication line. The acquired data are first pre-processed and then passed to the feature extraction algorithms which calculate a vector of features. Each feature, reflects a particular aspect of quality, therefore it is checked to verify whether the device satisfies the quality requirements. In case of discrepancy, the localization of tentative defects is performed. The entire application software is realized in LabVIEW.

3.1 Diagnostic stations

Functional decomposition of the diagnostic system was needed in order to stick to the test cycle, which is in our case 9s. It should be noted that major part of the test cycle is spent on motor handling and start-ups of the assessment session.

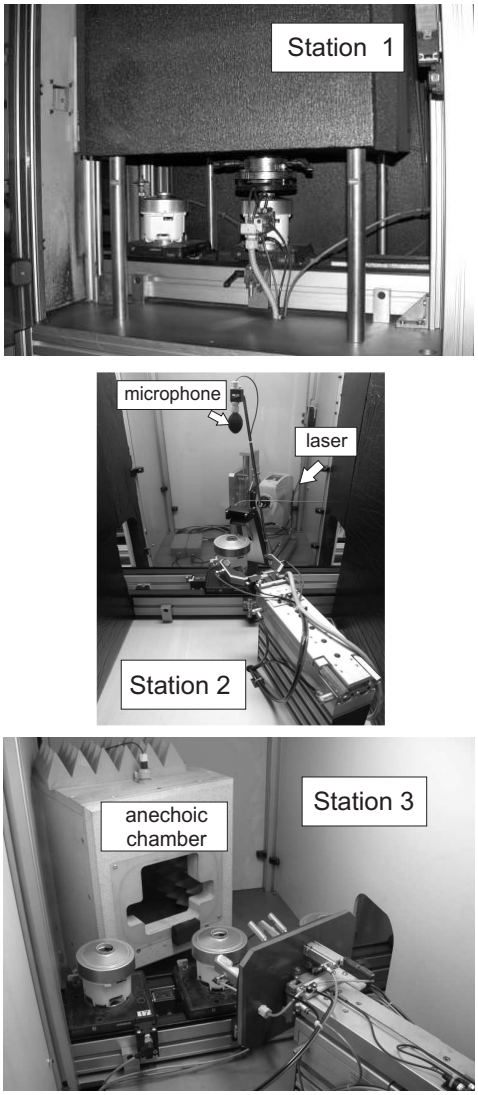

Fig. 7. Diagnostic stations for: (1) checking motor characteristic, (2) revealing problems with commutation, imbalance and aerodynamical faults, (3) diagnosing mechanical faults.

Diagnostic station 1

The primary role of the first station is to test the electrical characteristic of the motor under prescribed aperture of the intake. The characteristic data include electrical current, electrical power, pressure difference and revolution speed. The measurement conditions are fully supervised so that data corrections are performed in case of fluctuations in the environmental conditions. These include supplied voltage, air temperature and humidity. The corrected values are normalized with respect to the nominal supply voltage (230V) and standard atmospheric conditions.

Diagnostic station 2

The second station, shown in figure 7, serves for

- vibration measurements and imbalance detection,
- assessment of the quality of commutation, and
- diagnosis of mechanical faults that reflect in aerodynamical noise.

In order to precisely localize the source of imbalance, vibrations in radial directions are measured on two spots. Additional measurement is done on top of the housing in order to register vibrations in axial direction. Owing to the elaborated design of the gripper that grasp the motor during measurement sessions, the influence of vibrational disturbances from the assembly line and the environment are almost entirely attenuated. This technical detail turned to be one of the most demanding in the overall system design. Vibrations are acquired by laser vibrometer Ometron VQ-500-D. The vibrometer is fixed on a positioning mechanism, which allows for vertical movement of the vibrometer thus allowing measurement of vibrations in radial direction at two different spots. Measurements in the axial direction of the motor are carried out by using a mirror, which redirects the laser beam. Vibrations of the motor are evaluated by RMS values of 15 frequency bands 1kHz wide and ranging from 0 to 15kHz. For that purpose the vibration signal is sampled at the rate of 60kHz.

The quality of commutation is evaluated by measuring high-frequency disturbances in the supply voltage, which appear due to sparking between the brushes and collector bars. For that purpose a special device was developed Petrovčič et al. [2004]. The device operates as follows. First the high-frequency content is extracted out of the supply voltage. Then the envelope of the extracted signal is obtained. The envelope contains a chain of pulses, which correspond to the sparks intensity on the collector. Then the device generates a histogram of pulses with respect to the amplitudes. Finally, the assessment of commutation quality is done based on the shape of the histogram.

The aerodynamical noise produced by faulty motors with mechanical faults is most prominent at the nominal rotational speed of 800Hz. At this speed, the intensity of the noise emitted by the motor drowns out the erroneous sounds from the surroundings. It turns out, that by using a highly selective procedure described in section 2, one can carry out measurements in an open space without use of any anechoic chamber.

Diagnostic station 3

The third station serves for sound measurements and evaluation of mechanical faults which generate noise. It turns out that mechanical noise is the most prominent (best audible) at low rotational speed of 40Hz. Due to low sound intensity at the given speed, the measurements have to be carried out in an anechoic chamber in order to suppress the influence of disturbing noise from environment. The details on the procedures are given in section 2.

4. INTEGRATION OF THE DIAGNOSTIC SYSTEM WITH THE MES LEVEL

Current status

The assessment procedure results in a vector of features for every assembled motor. The feature vectors are stored in a SQL database hence allowing

- insight into the manufacturing history and
- support to the supervision of the entire production line.

The MSSQL application takes care of retrieval services for a broad spectrum of users such as operators, management staff and costumers. Having access to the data, customers are able to grasp all relevant statistics of the quality of the purchased products. This important human aspect of automation considerably contributes to the customer satisfaction and confidence in the manufacturer.

Further work

The next step of the diagnostic system integration into MES concerns realization of decision support to the production line monitoring (see figure 8). These modules are expected to allow for

- statistical quality control,
- early detection of trend changes on the production line and
- recognition of anomalous events.

The statistical quality control applied to the sequences of feature vectors serves to reveal changes in the statistics of the quality parameters. The patterns of modified statistical parameters are combined with the knowledge elicited from the operators and incrementally stored in a database of anomalous events on the assembly line. A dedicated inference module will perform early detection of the tentative anomalous events on the assembly line and isolation of the source by generating a list of the most suspected faults. This additional functionality will facilitate the design of the corrective actions.

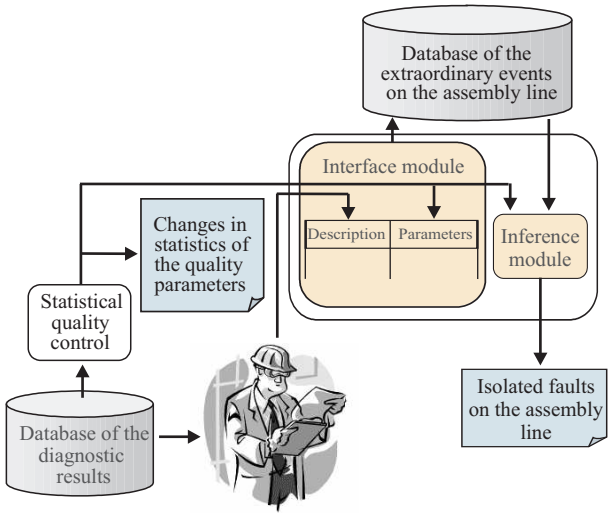

Fig. 8. The structure of the supervision support system

5. CONCLUSIONS

The paper presents the diagnostic system for on-line quality assessment of a new generation of electrical motors for vacuum cleaners. These motors are characterized by exceptional performance at decreased weight, which is result of novel design and plastic housing. In turn, it is almost impossible to perform their quality assessment "manually". Since its implementation the system performance proved exceptional so that more than 3 million motors have been tested so far.

The paper provides in-depth description of a part of the system, which serves for detection of mechanical faults on the basis of sound analysis. These faults occur most frequently. The proposed algorithms proved to be highly effective, robust and fast. The most attractive advantage of sound analysis is that measurements require no contact with the motor. It is worth highlighting that alternative means, such as current analysis and vibration analysis, failed to prove useful in this case. On the other hand, aerodynamical noise generated by a deformed fan-impeller are not reflected in current or vibration at all. Another aspect addressed in the paper is the possibility of system upgrade in terms of advanced production line supervision support. Nonetheless, it is important to stress that subject to minor adaptations, the system can be applied to a broader family of electrical motors.

6. ACKNOWLEDGEMENT

The support of the Slovenian Research Agency through grants L2-6554 and P2-0001 is gratefully acknowledged.

REFERENCES

E. Albas, T. Arikan, and C. Kuzkaya. In-process motor testing results using model based fault detection approach, 2006. URL `www.maintenanceworld.com/Articles/albasArikankuzkaya/emcw_2001_artesis_paper.pdf`.

U. Benko, J. Petrovčič, and Đ. Juričić. In-depth fault diagnosis of small universal motors based on acoustic analysis. In *Preprints of the 16th IFAC World Congress, 16th IFAC World Congress*, Prague, 2005.

Vogelsang & Benning. Routine test system for vacuum cleaner fans, 2007. URL `www.vogelsangbenning.de/en/index.html`.

S. Edwards, A.W. Lees, and M.I. Friswell. Fault diagnosis of rotating machinery. *Shock and Vibration Digest*, 30 (1):4–13, 1998.

J. Petrovčič, Đ. Juričić, and D. Tinta. *Detector and the apparatus for measurement of sparking intensity of commutator-based electric motors.* Patent no. 21381, Ljubljana, 2004.

R.B. Randall. *Frequency Analysis.* Brüel& Kjær, Denmark, 1987.

R.B. Randall. State of the art in monitoring rotating machinery. In *Proceedings of ISMA 2002*, volume 4, pages 1457–1477, Lueven, Belgium, September 2002.

Schenck. Testing and diagnostic system for vacuum cleaner blowers, 2007. URL `www.schenck-ind.com/balance4.html`.

T. Vetter, H. Weber, and J. Grossehelweg. Vollautomatische Fehlerdiagnose in der Serienfretigung von Elektromotoren, VDI-Tagung: "Überwachtung und Fehlerdiagnose", 1994. URL `VDI-Tagung: "berwachtung und Fehlerdiagnose"`.

Appendix A. EXTRACTION OF SIGNAL ENVELOPE BY USING ABSOLUTE VALUE

Amplitude modulated signal $y(t)$ can be written as

$$y(t) = [C + m(t)]\cos(\omega_c t) = y_e(t)\cos(\omega_c t)$$

where $y_e(t) = [C+m(t)]$ is a an envelope and $\omega_c = 2\pi/T_c$ is the carrier frequency. Let $\mathcal{F}\{y_e(t)\}(\omega) = 0 \;\; \forall\, |\omega| \geq \omega_{max}$ where $0 < \omega_{max} \ll \omega_c$. Fourier transform of $|y(t)|$ reads as

$$\mathcal{F}\{|y(t)|\}(\omega) = \sum_p \int_{T_p} y(t)e^{-i\omega t}dt - \sum_n \int_{T_n} y(t)e^{-i\omega t}dt = \\ = \mathcal{F}\{y(t)\}(\omega) - 2\sum_n \int_{T_n} y(t)e^{-i\omega t}dt\,. \quad \text{(A.1)}$$

T_p is one of p intervals where $y(t) \geq 0$ and T_n one of n intervals, where $y(t) < 0$ (see figure A.1). It holds that

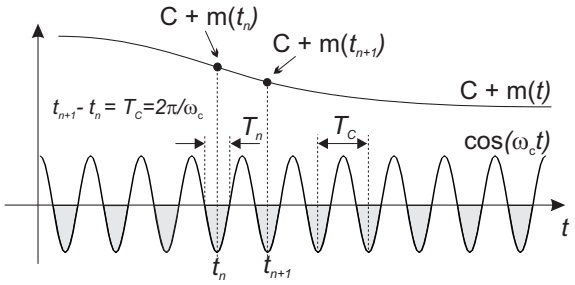

Fig. A.1. Schematic picture of a part of a modulated signal $\cos(\omega_c t)$ and the envelope $C + m(t)$. Shadowed intervals of the modulated signal are indicated by T_n, where $[C + m(t)]\cos(\omega_c t) < 0$.

$\mathcal{F}\{y(t)\}(\omega_0) = 0$ for $\omega_0 \in [0, \omega_{max})$, which results in simplification of equation A.1 to

$$\mathcal{F}\{|y(t)|\}(\omega_0) = -2\sum_n \int_{T_n} y(t)e^{-i\omega_0 t}dt = \quad \text{(A.2)}$$
$$= -2\sum_n \int_{T_n} [C + m(t)]\cos(\omega_c t)e^{-i\omega_0 t}dt\,.$$

In the limit case $\omega_c \to \infty$, $T_c \to 0$, the number of intervals $n \to \infty$ and the interval width $|T_n| = |T_c/2| \to 0$. As $|T_n| \to 0$, the term $[C + m(t)]e^{-i\omega_0 t}$ becomes constant in T_n and can be approximated by $[C + m(t_n)]e^{-i\omega_0 t_n} = y_e(t_n)e^{-i\omega_0 t_n}$ where t_n is the center of T_n (see figure A.1). The equation A.2 can be rewritten as

$$\lim_{\omega_c \to \infty} \mathcal{F}\{|y(t)|\}(\omega_0) = -2\sum_n^{\infty} y_e(t_n)e^{-i\omega_0 t_n} \int_{T_n = T_c/2} \cos(\omega_c t)dt = \\ = -2\sum_n^{\infty} y_e(t_n)e^{-i\omega_0 t_n}(-\frac{2}{\omega_c}) = \\ = 2\sum_n^{\infty} y_e(t_n)e^{-i\omega_0 t_n}\frac{T_c}{\pi}\,. \quad \text{(A.3)}$$

As $T_c \to 0 \Rightarrow |t_{n+1} - t_n| \to 0$. By replacing $\sum \to \int$, $T_c \to dt$, $t_n \to t$ equation A.3 reads as

$$\lim_{T_c \to 0} \mathcal{F}\{|y(t)|\}(\omega_0) = \frac{2}{\pi}\int y_e(t)e^{-i\omega_0 t}dt \quad \text{(A.4)}$$

which is nothing but a Fourier transform of $y_e(t)$ at frequency ω_0 multiplied by $2/\pi$. In real life, $\omega_c < \infty$ and only approximation of A.4 holds. So, if $\omega_0 \ll \omega_c$, then $\mathcal{F}\{|y(t)|\}(\omega_0) \propto \mathcal{F}\{y_e(t)\}(\omega_0)$.